Magnetic and magneto-optical quenching in (Mn^{2+}, Sr^{2+}) metaphosphate glasses

A. Winterstein,[1] H. Akamatsu,[3] D. Möncke,[1] K. Tanaka,[2] M. A. Schmidt,[3] and L. Wondraczek[1,*]

[1]*Otto-Schott-Institute, University of Jena, Jena, Germany*
[2]*Department of Material Chemistry, Graduate School of Engineering, Nishikyu-ku Kyoto University, Kyoto, Japan*
[3]*Department of Fiber Optics, Institute of Photonic Technology, Jena, Germany*
**lothar.wondraczek@uni-jena.de*

Abstract: Transition metal ions such as Mn^{2+}, Fe^{2+}, or Co^{2+} provide an interesting alternative to rare earth dopants in optically active glasses. In terms of their magneto-optical properties, they are not yet very well exploited. Here, we report on the effect of Mn^{2+} on Faraday rotation in a metaphosphate glass matrix along the join $Mn_xSr_{1-x}(PO_3)_2$ with x = 0...1. Mn^{2+} shows small optical extinction in the visible spectral range and, compared to other transition metal ions, a high effective magnetic moment. At high Mn- levels, however, the magneto-optical activity of Mn^{2+} is strongly quenched due to ionic clustering. The magnetic properties of the heavily Mn^{2+}-loaded phosphate matrix are dominated by a superexchange interaction in the Mn^{2+}-O-Mn^{2+} bridge with antiparallel spin alignment between Mn^{2+} and O^{2-} species. The apparent paramagnetic potential of Mn^{2+} species can therefore not be exploited at room temperature.

OCIS codes: (160.2750) Glass and other amorphous materials; (160.3820) Magneto-optical materials.

References and links

1. J. Qiu and K. Hirao, "The Faraday effect in diamagnetic glasses," J. Magn. Reson. **13**(05), 1358–1362 (1998).
2. Landolt-Börnstein, *Numerical Data and Functional Relationships in Science and Technology* New Series, III/19, Subvolumes a to i2, Magnetic Properties of Metals (Springer-Verlag, Heidelberg, 1986–1992).
3. Landolt-Börnstein, *Numerical Data and Functional Relationships in Science and Technology* New Series, II/2, II/8, II/10, II/11 and II/12a, Coordination and Organometallic Transition Metal Compounds (Springer-Verlag, Heidelberg, 1966–1984).
4. *Tables de Constantes et Données Numérique*, Relaxation Paramagnetique (Masson, Paris, 1957), Vol. 7.
5. J. J. Rhyne and T. R. McGuire, "Magnetism of rare-earth elements, alloys, and compounds," IEEE Trans. Magn. **8**(1), 105–130 (1972).
6. C. Zener, "Interaction between the d-shells in the transition metals. III. Calculation of the Weiss factors in Fe, Co, and Ni," Phys. Rev. **83**(2), 299–301 (1951).
7. C. Kittel, *Einführung in die Festkörperphysik* (Oldenburg Verlag, 1995).
8. H. Akamatsu, S. Oku, K. Fujita, S. Murai, and K. Tanaka, "Magnetic properties of mixed-valence iron phosphate glasses," Phys. Rev. B **80**(13), 134408 (2009).
9. R. Reisfeld, A. Kisilev, and C. K. Jørgensen, "Luminescence of manganese(II) in 24 phosphate glasses," Chem. Phys. Lett. **111**(1–2), 19–24 (1984).
10. R. Verhelst, R. Kline, A. de Graat, and H. Hooper, "Magnetic properties of cobalt and manganese aluminosilicate glasses," Phys. Rev. B **11**(11), 4427–4435 (1975).
11. J. Pommier, J. Ferré, and S. Senoussi, "Origin of the Faraday effect in a transparent magnetic Mn^{2+} glass," J. Phys. C Solid State Phys. **17**(31), 5621–5633 (1984).
12. W. Nägele, K. Knorr, W. Prandtl, P. Convert, and J. L. Buevoz, "Neutron scattering study of spin correlations and phase transitions in amorphous manganese aluminosilicates," J. Phys. C Solid State Phys. **11**(15), 3295–3305 (1978).
13. K. Knorr, R. Geller, and W. Prandl, "Mössbauer and neutron diffraction investigations of magnetic effects in $Fe_2Ca_3Si_3O_{12}$ and $Al_2Mn_3Si_3O_{12}$ glasses," J. Magn. Magn. Mater. **4**(1-4), 258–261 (1977).
14. J. Ferré, J. Pommier, J. P. Renard, and K. Knorr, "Magnetic properties of an amorphous insulating spin glass: manganese aluminosilicate," J. Phys. C Solid State Phys. **13**(19), 3697–3711 (1980).

#180576 - $15.00 USD Received 26 Nov 2012; revised 3 Jan 2013; accepted 7 Jan 2013; published 8 Jan 2013

15. G. C. Lau, T. Klimczuk, F. Ronning, T. M. McQueen, and R. J. Cava, "Magnetic properties of the garnet and glass forms of $Mn_3Al_2Si_3O_{12}$," Phys. Rev. B **80**(21), 214414 (2009).
16. H. Akamatsu, K. Fujita, S. Murai, and K. Tanaka, "Magneto-optical properties of transparent divalent iron phosphate glasses," Appl. Phys. Lett. **92**(25), 251908 (2008).
17. E. H. Williams, "The magnetic properties of some rare earth oxides as a function of the temperature," Phys. Rev. **12**(2), 158–166 (1918).
18. M. Yamane and Y. Asahara, *Glasses for Photonics* (Cambridge University Press, 2005).
19. M. A. Schmidt, L. Wondraczek, H. W. Lee, N. Granzow, N. Da, and P. St. J. Russell, "Complex Faraday rotation in microstructured magnetooptical fiber waveguides," Adv. Mater. **23**(22-23), 2681–2688 (2011).
20. C. B. Rubinstein, S. B. Berger, L. G. Van Uitert, and W. A. Bonner, "Faraday rotation of rare-earth (III) borate glasses," J. Appl. Phys. **35**(8), 2338–2340 (1964).
21. N. Da, M. Peng, S. Krolikowski, and L. Wondraczek, "Intense red photoluminescence from Mn^{2+}-doped (Na^+; Zn^{2+}) sulfophosphate glasses and glass ceramics as LED converters," Opt. Express **18**(3), 2549–2557 (2010).
22. I. Konidakis, C. Varsamis, E. I. Kamitsos, D. Möncke, and D. Ehrt, "Structure and properties of mixed strontium-manganese metaphosphate glasses," J. Phys. Chem. C **114**(19), 9125–9138 (2010).
23. D. Möncke, E. I. Kamitsos, A. Herrmann, D. Ehrt, and M. Friedrich, "Bonding and ion–ion interactions of Mn^{2+} ions in fluoride-phosphate and boro-silicate glasses probed by EPR and fluorescence spectroscopy," J. Non-Cryst. Solids **357**(14), 2542–2551 (2011).
24. N. Zotov, H. Schlenz, B. Brendebach, H. Modrow, J. Hormes, F. Reinauer, R. Glaum, A. Kirfel, and C. Paulmann, "Effects of MnO-doping on the structure of sodium metaphosphate glasses," Z. Naturforsch. **58a**, 419–428 (2003).
25. R. K. Brow, "Review: the structure of simple phosphate glasses," J. Non-Cryst. Solids **263–264**, 1–28 (2000).
26. P. A. Bingham and R. J. Hand, "Sulphate incorporation and glass formation in phosphate systems for nuclear and toxic waste immobilization," Mater. Res. Bull. **43**(7), 1679–1693 (2008).
27. P. C. Schultz, "Optical absorption of the transition elements in vitreous silica," J. Am. Ceram. Soc. **57**(7), 309–313 (1974).
28. G. Gao, S. Reibstein, M. Peng, and L. Wondraczek, "Dual-mode photoluminescence from Mn^{2+}-doped Li,Zn-aluminosilicate glass ceramics," Phys. Chem. Glasses: Eur. J. Glass Sci. Technol. B **52**(2), 59–63 (2011).
29. H. Akamatsu, K. Tanaka, K. Fujita, and S. Murai, "Spin dynamics in oxide glass of Fe_2O_3–Bi_2O_3–B_2O_3 system," J. Magn. Magn. Mater. **310**(2), 1506–1507 (2007).
30. N. Wiberg, E. Wiberg, and A. F. Holleman, *Lehrbuch der Anorganischen Chemie* (Walther de Gruyter, 2007).
31. S. J. M. Liu, *Photonic Devices* (Cambridge University Press, 2009).
32. J. H. Van Vleck and M. H. Hebb, "On the paramagnetic rotation of tysonite," Phys. Rev. **46**(1), 17–32 (1934).
33. S. H. Lin and H. Eyring, "Magneto-optical rotation of transition metal complexes," J. Chem. Phys. **42**(5), 1780–1784 (1965).

1. Introduction

Magneto-optics utilize the Faraday effect, by which the plane of linearly polarized light is rotated as the light propagates through a magneto-optical (MO) medium which is exposed to a longitudinal magnetic field. The angle of polarization rotation (denoted Faraday angle) is proportional to the magnetic field strength, the medium length and the Verdet constant V which is a material parameter. By definition, V is positive for diamagnetic and negative for paramagnetic or antiferromagnetic materials. Most glasses are weakly diamagnetic [1]. However, if strongly paramagnetic ions are incorporated in sufficiently high concentration into a weakly diamagnetic matrix, a significant Faraday rotation can be achieved. The governing factor in this process is the magnetic susceptibility, χ, of the dopant. The value of χ depends strongly on the employed active species and may range from ~10^1 for typical diamagnetic species, to ~10^3 for transition metal (TM) ions up to ~10^4 for rare earth (RE) ions [2–4]. The effective magnetic moment μ_{eff} is usually also smaller for TM than for RE species. In a multicomponent medium, the contributions of individual dia- and paramagnetic nuclei usually add up. In a first approximation, a linear mixing rule may be assumed for this, where $V = n_{\text{dia}}V_{\text{dia}} + n_{\text{para}}V_{\text{para}}$, with the molar fraction n_i of para- and diamagnetic species, and the Verdet constant V_i of each species. The straightforward approach in the preparation of highly paramagnetic glasses is therefore to find a suitable matrix glass in which very high levels of paramagnetic species can be incorporated without initiating chemical phase separation. However, also strongly nonlinear mixing effects have frequently been observed in the past [5].

Compared to the *f*-shells of RE ions, the *d*-shells of TM ions are not isolated from their environment. Therefore, the electronic properties of a TM ion depend strongly on the ligand field. Four types of magnetic coupling may occur in first row TM oxides [6]: (*i*) direct

#180576 - $15.00 USD Received 26 Nov 2012; revised 3 Jan 2013; accepted 7 Jan 2013; published 8 Jan 2013

exchange between incomplete *d*-shells of nearest neighbors, (*ii*) spin coupling between inner *d*-electrons and electrons of the conduction band of the host, which, since unpopulated at room temperature, can be neglected in glasses, (*iii*) kinetic coupling of conduction electrons, and (*iv*) the so-called superexchange through an intermediate species. Other effects, such as the configurational occupation of degenerated twofold and threefold energy levels of *d*-orbitals (high/low spin states) may additionally influence the magnetic and magneto-optical properties of TM ions in a solid matrix. In an oxide lattice, superexchange is typically the dominant coupling mechanism. For example, the interaction of the *d*-shells of Mn^{2+} with the *p*-orbitals of the O^{2-} ligands usually leads to an antiferromagnetic (AFM) behavior. In crystalline MnO, this is caused by the antiparallel alignment of spins in the Mn^{2+}-O-Mn^{2+} bridge [7]. Most of the divalent TM compounds show AFM behavior, e.g. MnO, CoO, FeO, and NiO [8,9].

TM containing glasses have been studied in detail for their magnetic properties [10–15]. On the other hand, their magneto-optical (MO) properties remain - qualitatively as well as quantitatively - poorly understood and today's MO applications rely solely on RE (Tb^{3+}) loaded glasses [16–20]. This may at least partially be related to the difficulty of finding a suitable matrix material in which the TM species can be stabilized in the desired valence state, coordination number and molar quantity, and which still exhibits a wavelength range with sufficient optical transparency for a magneto-optical application. Here, phosphate glasses with their typically low optical dispersion, elevated refractive index, high Abbé number, broad transmission window provide an interesting alternative. Most importantly, high levels of TM oxides can be incorporated into these glasses [21–25]. In addition, with only a few exceptions [21,22], most phosphate glasses provide a rather acidic environment in which many polyvalent ions can be stabilized in their lower redox states [22,23]. TM-oxide containing phosphate glasses exhibit even at high doping levels reasonable luminescence behavior without showing the same quenching effects so common in other glass compositions (e.g [22,23].). Other studies showed that high levels of TM addition can favorably affect the mechanical properties or the corrosion resistance of phosphate glasses [26]. Addition of paramagnetic transition metal ions such as Mn^{2+}, Fe^{2+}, or Co^{2+} is also known to affect the magnetic suscibility, antiferromagnetic behavior and magneto-optical properties of the glass [8,10,14]. However, while most studies or even applications which utilize magnetic properties of glasses do not require high optical transparency, even minor amounts of coloring species may have a devastating effect on the magneto-optical performance of the material. To account for this and to evaluate and compare different materials, a figure of merit (FOM) has been defined as the Faraday rotation relative to the spectral absorption α of the material, FOM = V/α. Contrary to RE-based materials in which the active species is usually present in only a single valence state, in TM-containing materials, redox pairs such as Mn^{2+}/Mn^{3+} and Fe^{2+}/Fe^{3+} have to be considered. In order to obtain a material with high FOM and, hence, high transparency in the UV-visible spectral range, the redox equilibrium must be shifted completely to the divalent state for Mn^{2+}. In the case of iron, only Fe^{2+} provides notable Faraday rotation, but also absorbs strongly between 600 and 1800 nm [6,27]. Careful balancing is therefore required between optical absorption and Faraday rotation [7,8].

Because Mn^{2+} exhibits one of the highest theoretical magnetic moments of all ion species of the TM group, we focus here on the join of $MnPO_3$-$SrPO_3$ which shows excellent glass formation even at very high Mn^{2+} content.

2. Experimental

Glasses of the series $Mn_xSr_{1-x}(PO_3)_2$ with x = 0; 0.01; 0.1; 0.2; 0.4; 0.5; 0.6; 0.8 and 1.0 were prepared by melting 50 g batches of the raw materials $MnCO_3$, $Sr(H_2PO_4)_2$ and $NH_4H_2PO_4$ in an inductively heated furnace. To prevent the oxidation of Mn^{2+} species, a reducing atmosphere was established during melting, using alumina crucibles which were placed within SiC-C jackets. As atmospheric oxygen reacts with the crucible jackets to form CO, the

#180576 - $15.00 USD Received 26 Nov 2012; revised 3 Jan 2013; accepted 7 Jan 2013; published 8 Jan 2013

ensuing atmosphere in the vicinity of the melt is sufficiently depleted of oxygen to prevent oxidation of Mn^{2+} ions. The raw materials were homogeneously mixed in a tumbling drum and fed into the crucible, which was preheated to 700°C for 30 min of initial calcination. The temperature was then raised to the fining temperature of 1150°C, where the melt was kept for 20 min before casting into preheated (450°C) graphite moulds. Annealing lasted for 60 min at this temperature before the samples were cooled down to room temperature at a rate of ~2 K/min. Optical transmission spectra were recorded on 1.5 to 3 mm thick, polished, plane parallel sample plates over the range from 200 to 2500 nm with an UV-VIS spectrophotometer, equipped with a 150 mm integration sphere (Lambda 950, Perkin Elmer). Spectra were corrected for reflection loss, normalized, and deconvoluted into Gaussian absorption peaks. The Faraday rotation was also measured on the polished sample plates at room temperature (25°C) over the spectral range of 350 to 850 nm and using a magneto-optical analyzer working at a constant magnetic field strength of 1.5 T (K-250, Jasco). The change in the polarization angle was detected with a precision of 0.005°. The magnetic properties of the samples with $x = 0.5$ and $x = 1.0$ were analyzed on powder specimens which were fixed on a non-magnetic polymer sample holder. The temperature dependence of dc and ac susceptibilities was determined with a superconducting quantum interference magnetometer over the temperature range of 1.8 - 300 K (MPMS-XL, Quantum Design). A temperature step-size of 0.1 K was employed in the temperature range of 1.8 - 5 K, 0.5 K for 5 – 10 K, 1 K for 10 – 50 K, and 10 K for 50 – 300 K using field strengths of 0.0 T as reference and of 0.1 T. The data thus obtained were normalized in regard to the sample weight and molar mass.

3. Results and discussion

The glass network of metaphosphate glasses of the join $MnPO_3$-$SrPO_3$ is based on polymer-like chains of phosphate tetrahedra with two bridging and two terminal oxide ions, the Q^2 structural units $[PO_2O_{2/2}]^-$ [22,24,25]. These chains are cross-linked to a higher or lesser extent by the modifier cations. Detailed information on the structure of these glasses is provided in [22]. X-ray diffraction (XRD) was used to confirm that the samples are amorphous as only a broad undefined glass hump is observed for all glasses of the series. No further sharpening of this glass hump is evident for MnO rich samples.

3.1 Absorption spectroscopy

With increasing Mn^{2+} content, the glass samples displayed an increasingly orange tint (Fig. 1). This tint is attributed to Mn^{2+} species which show relatively sharp absorption bands around 350 and 415 nm. Furthermore, a weaker broad shoulder extends from the second band up to 550 nm. The assignments of the different bands to electronic d-d transitions of Mn^{2+} and Mn^{3+} follow the detailed discussion found in [22] for the very same glass system. Photoluminescence spectroscopy revealed in the orange to red emission which is typical for octahedrally coordinated Mn^{2+} (while green emission typically indicates tetrahedrally coordinated Mn^{2+}) [21–23,28]. This information is the more important, as the electronic ground state $^6A_1(S)$ for d^5 ions is identical for the tetrahedral and octahedral field. Mn^{2+} ions take in an oxide environment the high-spin configuration and due to a lack of excited spin sextet terms are all transitions not only Laport forbidden, like all d-d transitions, but additionally also spin-forbidden. This explains the very small molar extinction coefficients of only ~0.2 $Lmol^{-1}cm^{-1}$ [21,22]. In comparison, the molar extinction coefficient of the spin allowed d^4 ion Mn^{3+} is several orders of magnitude higher: even very small traces of Mn^{3+} can have a strong impact on the absorption spectra and give Mn-doped glasses the typical dark violet to blackish color.

Optical absorption spectroscopy was conducted to quantify the ratio of $Mn^{2+}/(Mn^{2+} + Mn^{3+})$, as required for the determination of the magneto-optical FOM. The collected UV-VIS absorption spectra are shown in Fig. 1(a). For $x = 0$, the UV absorption edge occurs at a

#180576 - $15.00 USD Received 26 Nov 2012; revised 3 Jan 2013; accepted 7 Jan 2013; published 8 Jan 2013

wavelength below 300 nm. With increasing x, the bands at 353 and 414 nm gradually increase in intensity for the whole glass series up to x = 1. The shallow orange tail increases analogously in intensity, although small differences in the position of the band maximum indicate another contribution. That is, the d-d transitions of Mn^{2+} near 440 nm and 540 nm are overlaid by three strong d-d transitions of Mn^{3+} between 470 and 660 nm. Figure 1(b) shows the Gaussian deconvolution of the absorption spectra which reveals the exact peak positions of all optical transitions for the sample with x = 1. The spectra are in good agreement with those shown in [22] where the ligand field splitting Dq = 845 cm^{-1} and the Racah interelectronic repulsion parameter B = 756 cm^{-1} confirmed that the coordination of Mn^{2+} is primarily octahedral and that the outer electrons are configured in the high spin state [22].

The fraction of Mn^{3+} was calculated from the intensity of the strongest absorption band near 500 nm using the Lambert-Beer law, using an extinction coefficient of 25 $Lmol^{-1}cm^{-1}$ [22]. In this way, it was confirmed that the concentration of Mn^{3+} is indeed very low, i.e. < 0.1% of the total Mn-content. Its influence on the MO properties and the corresponding FOM was therefore ignored in the following discussion.

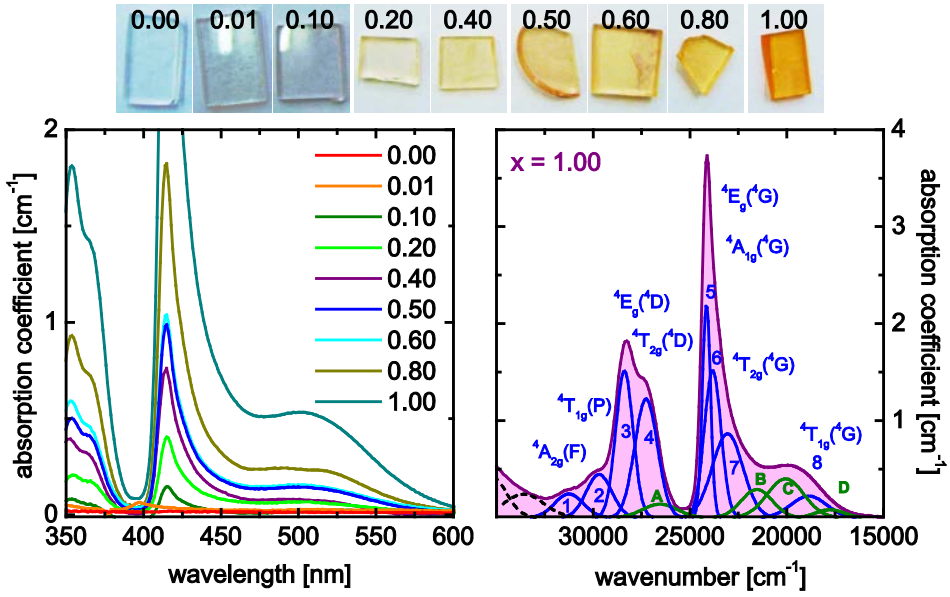

Fig. 1. (a) UV-VIS optical absorption of $Mn_xSr_{1-x}(PO_3)_2$ glasses normalized to sample thickness. (b) Exemplary Gaussian deconvolution of the data for the sample with x = 1, dots represent the experimental, lines the fitted spectrum. Labels in (b) indicate the active electronic level for each transition; transitions A-D are assigned to residual Mn^{3+}-species. Photographs of each sample are displayed above the spectra.

3.2 Magnetic properties

The magnetic properties of the glasses were studied as a basis for understanding the MO behavior. Susceptibility data for x = 0, 0.5, and 1.0 are plotted in Fig. 2. Paramagnetic behavior over the whole temperature range is observed for all Mn-containing samples. Since field-cooled and zero-field cooled scans coincide with each other within the temperature range of 2 to 10 K and AC measurements did not reveal any frequency dependence of the magnetic behavior, spin glass behavior can be excluded for all temperatures above 1.8 K.

The molar susceptibilities increase with decreasing temperature for x = 0.5 and 1. For x = 0, the typical diamagnetic behavior is observed with only a weak temperature dependence of the susceptibility. While in the high-temperature regime, a somewhat lager χ is found for x = 1

#180576 - $15.00 USD Received 26 Nov 2012; revised 3 Jan 2013; accepted 7 Jan 2013; published 8 Jan 2013

as compared to x = 0.5, an equivalence occurs at ~55 K. In the low temperature regime, the magnitude of χ is significantly higher for x = 0.5.

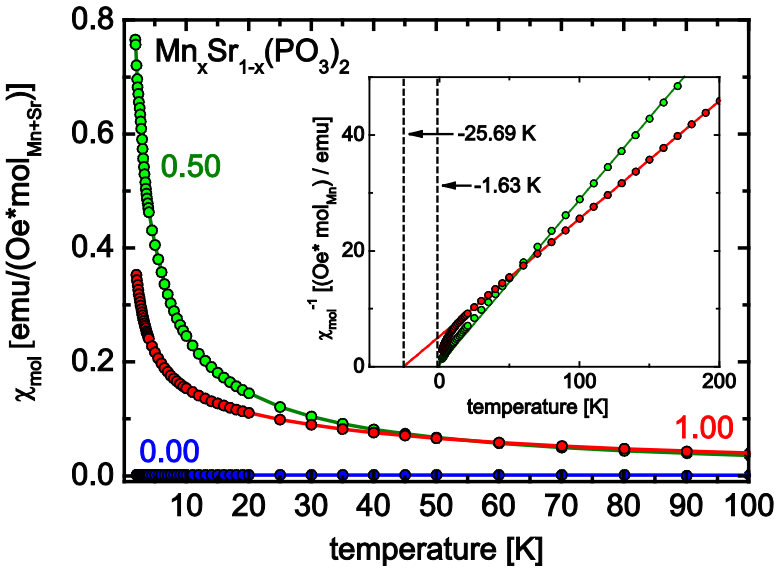

Fig. 2. Molar susceptibility as a function of temperature for $Mn_xSr_{1-x}(PO_3)_2$ glasses. The inverse molar susceptibility and the graphical determination of the Weiss temperature θ_W are shown in the inset.

In order to investigate the magnetic interactions between the Mn^{2+} ions, the inverse susceptibility is considered in more detail (inset of Fig. 2). For antiferromagnetic materials, the maximum magnetic susceptibility is reached at the Néel temperature T_N, the temperature above which an antiferromagnetic or ferrimagnetic material becomes paramagnetic. For crystalline MnO T_N is 116 K [29]. Since pure MnO is antiferromagnetic due to the predominance of Mn^{2+}-O-Mn^{2+} antiferromagnetic interaction, it is assumed that glasses exhibit paramagnetic behavior which might have additional antiferromagnetic contributions [30]. Relative to a (fictive) crystal of equivalent chemical composition, in disordered systems, T_N shifts to lower values. Moreover, in the present case, the concentration of Mn^{2+} is lower than in MnO crystals and freezing of randomly oriented magnetic moments should be observed therefore at again lower temperatures [7,10,29]. No magnetic transition is apparent in the studied glass system as Fig. 2 shows no maximum of the magnetic susceptibility or Néel temperature, just as AC and DC measurements exclude spin glass behavior for temperatures above 1.8 K. Possibly, the Néel temperature will be found at even lower temperatures. Above the Néel temperature, the susceptibility of an antiferromagnetic system shows Curie-Weiss paramagnetic behavior. The Curie-Weiss law describes the magnetic susceptibility χ of a ferromagnetic material in the paramagnetic region above the Curie temperature T_C. For temperatures $T >> T_C$, the Weiss temperature θ_w, which is somewhat higher than the Curie point, is used instead of T_C:

$$\frac{1}{\chi} = \frac{T - \theta_W}{C} \tag{1}$$

where χ is the magnetic susceptibility, T the absolute temperature in K and C the Curie constant with

$$C = \frac{N\mu_{eff}^2}{3k_B} \tag{2}$$

#180576 - $15.00 USD Received 26 Nov 2012; revised 3 Jan 2013; accepted 7 Jan 2013; published 8 Jan 2013

where N is the Avogadro number, k_B is the Boltzmann constant and μ_{eff} the effective magnetic moment, which is defined as $\mu_{eff} = 2[S(S + 1)]^{1/2}\ \mu_B$ [7] with the total spin angular momentum S and the Bohr magneton μ_B. In cases of high high-spin d^5 complexes such as Mn^{2+} the ground state of should have a magnetic moment close to the spin-only value of ~5.92 μ_B, since an S-term carries no angular momentum [7]. The effective magnetic moment in the studied samples, estimated by rearranging Eq. (2), yielded values of $5.32\mu_B$ and $6.22\mu_B$, for the sample with $x = 0.5$ and $x = 1$, respectively. For $x = 0.5$, μ_{eff} is lower than the value for the free ion while for $x = 1$ μ_{eff} is somewhat higher. Similar deviations are known from other glass systems [10,16]. The value of μ_{eff} depends strongly on the spin state and the coordination of the TM. For octahedral high spin complexes of Mn^{2+}, the orbital moments in the ligand field are effectively quenched, which could have a strong influence on the susceptibility, especially in the low temperature regime, and thus explain the higher value of μ_{eff} for $x = 1$ [7]. For $x = 0.5$, the influence of Sr^{2+} ions on the coupling mechanism has to be considered as well, especially since a mixed cation effect was previously observed in the SrO-MnO-phosphate system [22].

At lower temperature, Fig. 2 shows a deviation of the magnetic susceptibility from linear behavior. This can be interpreted as a result of short-range order antiferromagnetic correlation. The absolute value of the Weiss temperature $|\theta_W|$ provides a measure of the magnitude of the magnetic interactions. The values of θ_W and C were estimated by linear extrapolation of the $\chi^{-1}(T)$ data to $\chi^{-1} = 0$ and θ_W values of –2 K and –26 K were obtained for $x = 0.5$ and $x = 1$, respectively. The negative Weiss temperature confirms the antiferromagnetic behavior. As mentioned before, for the glasses with $x = 0.5$ and $x = 1$, AC measurements showed no magnetic transitions for temperatures as low as 1.8 K, which is lower than one tenth of $|\theta_W|$. This indicates that the emergence of long-range magnetically ordered states is suppressed due to some type of magnetic frustration.

The strong antiferromagnetic coupling between Mn^{2+} ions in crystalline MnO has been mentioned before. The fact that similar effects are weaker in MnO-containing glasses can be explained by the structure of MnO clusters in metaphosphate glasses compared to MnO crystals. It has been shown previously by electron paramagnetic resonance spectroscopy that magnetic coupling becomes dominant when the distance between Mn^{2+} ions falls below ~4 Å [23]. Possible configurations of neighboring MnO-octahedra are depicted in Fig. 3. The corresponding Mn-Mn distances are slightly higher than 3 Å in edge-sharing MnO octahedra, which is reflected in an exchange narrowing of the main EPR resonance at g ~2 [23]. In $SrMn(PO_3)_2$ glasses, increasing MnO levels cause the formation of MnO clusters built from an increasing number of corner-sharing MnO octahedra, for which the Mn-Mn distance never falls below 4 Å [22] (for comparison, crystalline MnO comprises edge-sharing MnO octahedra with a Mn-Mn-distance of ~3 Å). From this, we conclude that direct interaction between neighboring Mn^{2+} species is not expected to contribute significantly to the magnetic and MO behavior of the present material. Assuming a statistical distribution of Mn^{2+} ions in the glassy matrix, the distances between the ions would result directly from their volumetric concentration. Then, volumetric concentrations of Mn^{2+} of $\sim 4.63 \cdot 10^{21}$ cm^{-3} for $x = 0.5$ and $\sim 8.61 \cdot 10^{21}$ cm^{-3} for $x = 1$, result in Mn-Mn distances of ~6.0 Å and ~4.9 Å, respectively. Noteworthy, however, the Mn^{2+} distribution is not simply statistical. That is, in metaphosphate glasses clusters of corner-sharing MnO octahedra may form already at low dopant concentration [22].

#180576 - $15.00 USD Received 26 Nov 2012; revised 3 Jan 2013; accepted 7 Jan 2013; published 8 Jan 2013

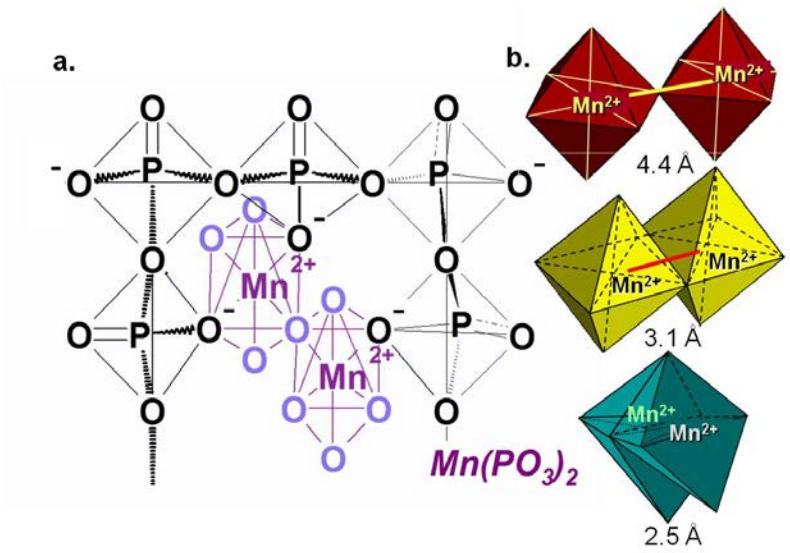

Fig. 3. Schematic of the structure of manganese metaphosphate (*a*) and individual clusters of MnO_6 octahedra (*b*, from top to bottom: corner-sharing, edge-sharing, face-sharing).

3.3 Magneto-optical quenching

Figure 4 displays the obtained Verdet constant as a function of wavelength for x = 0, 0.5 and 1.0. The value of V follows a quadratic decay function. For the un-doped matrix glass of $Sr(PO_3)_2$, V = 7.4 rad T^{-1} m^{-1} at a wavelength of 500 nm. With increasing Mn^{2+} content, the paramagnetic contribution increases and the overall Faraday rotation decreases to a value of V = 6.05 rad T^{-1} m^{-1} at 500 nm for x = 1. The individual paramagnetic contribution can be estimated by subtracting the diamagnetic baseline of x = 0 from the data obtained for higher x. For x = 1 the paramagnetic contribution V_{para} is about –3.6 rad T^{-1} m^{-1} to –0.03 rad T^{-1} m^{-1} in the wavelength range between 350 to 850 nm. For comparison, commercial Tb^{3+}-based phosphate glasses exhibit a V value of up to –93 rad T^{-1} m^{-1} (room-temperature, 500 nm [31]). For x = 0.5, a somewhat higher positive FOM is achieved compared to x = 1 since the optical transmission of this glass is higher although the paramagnetic contribution is lower.

A simple assumption for the value of V at lower temperatures can be derived from the measurements of the low-temperature magnetic behavior, since the paramagnetic Verdet constant is proportional to χ, connected through a material constant [19]. Given the fact that the susceptibility values increase from room temperature to lower temperatures by a factor of 10 (at a temperature of ~5 K), similar behavior may be expected for the paramagnetic contribution to the overall Faraday rotation. According to van Vleck and Hebb [32], the value of V depends also on the electronic transition probability and the transition wavelength λ_t. Plotting the inverse Verdet constant over λ^2 gives rise to an almost linear relation between the two quantities (Fig. 5). This plot describes the paramagnetic rotation, with the assumption that the Faraday rotation is derived from only one electronic transition at λ_t. In this case, λ_t reflects the weighted average of all actual transition wavelengths. The relative strength and proximity of the transitions are neglected. The value is easy to obtain when one transition is dominant. If several transitions are involved in the Faraday effect, this value can serve as an indicator of the spectral region in which the transition is located [20]. The apparent transition wavelength can be derived from the slope and horizontal intercept of the Van Vleck plot. For the studied glasses, a shift to higher wavelengths is observed, i.e., from ~250 nm for x = 0.5 to ~330 nm for x = 1. This is in agreement with the stronger paramagnetic effect for x = 1 at room temperature as this sample shows the stronger increase in the slope plotted in Fig. 5. For the

#180576 - $15.00 USD Received 26 Nov 2012; revised 3 Jan 2013; accepted 7 Jan 2013; published 8 Jan 2013

present glass, λ_t and all transition wavelengths lie below the UV edge and will not be discussed further. However, quenching of V is related to the already discussed superexchange mechanism. As the contribution of the magnetic moment for high spin states of octahedral Mn^{2+} (ground state $^6A_{1g}$) is quenched, very different susceptibility and rotation behaviors are observed for the samples with $x = 0$ and $x = 1$.

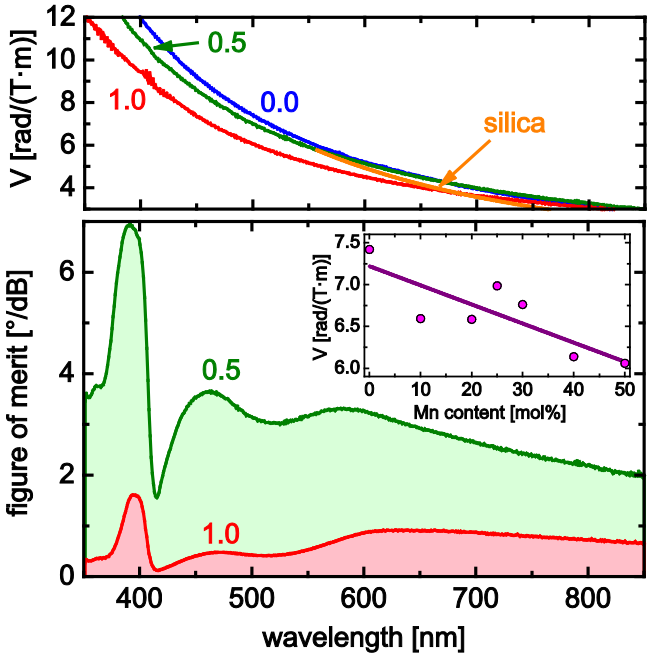

Fig. 4. Verdet constant of $Mn_xSr_{1-x}(PO_3)_2$ glasses for x = 0, 0.5 and 1.0 as obtained at room temperature and corresponding FOM. The inset depicts the linear fit of V at a wavelength of 500 nm to the molar content of Mn^{2+} in comparison to vitreous SiO_2 [20].

For Mn^{2+} (d^5) high spin complexes, the magnetic moment does not manifest since the ground state in both octahedral and tetrahedral coordination constitutes an A_g-and no T_g-term, but only T_g – terms yield a net magnetic contribution [33]. On the other hand, for low spin octahedral complexes, participation of the effective magnetic moment in the Faraday rotation could indeed occur since these complexes have a $^3T_{2g}$ ground state. Consequently, higher values of V could develop in the presence of a very strong ligand field and, hence, high $\Delta_0/10D_q$. Therefore, other glass compositions with high Mn^{2+} concentration could be considered to improve the rotation characteristics.

#180576 - $15.00 USD Received 26 Nov 2012; revised 3 Jan 2013; accepted 7 Jan 2013; published 8 Jan 2013

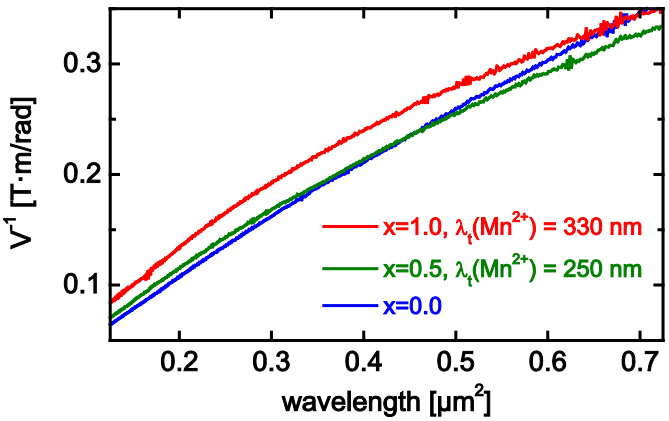

Fig. 5. Inverse Verdet constant as a function of the squared transition wavelength (van Vleck - plot, data obtained at room temperature).

4. Conclusions

In summary, metaphosphate glasses along the join $Mn_xSr_{1-x}(PO_3)_2$ with x = 0...1. Mn^{2+} were investigated for their magnetic and magneto-optical properties. In these glasses, the matrix is dominated by Q^2 phosphate groups. Mn^{2+} species are present in octahedral coordination with a statistical interionic distance of about 5 - 6 Å, though cluster formation may occur even for low MnO levels and result in effective distances of only ~4 Å. The magnetic interactions between Mn^{2+} ions are antiferromagnetic, as revealed by a negative Weiss temperature. The magnitude of Faraday rotation was shown to depend strongly on superexchange interaction through Mn^{2+}-O-Mn^{2+} bridges. In addition, the magneto-optical properties are strongly quenched due to a non-magnetic ground state (A_g – term) and spin forbidden transitions. For these reasons, the overall paramagnetic contribution of Mn^{2+} remains small as compared to the diamagnetic rotation of the phosphatic matrix itself. Comparing the magnetic properties with the magneto-optical properties lets us expect a significantly stronger paramagnetic rotation at temperatures below 50 K. On the other hand, heavily Mn^{2+}-loaded glasses could be also designed as zero-rotation materials.

Acknowledgment

We gratefully acknowledge technical support with glass melting by Dr. Ralf Keding of MPL Erlangen.

#180576 - $15.00 USD Received 26 Nov 2012; revised 3 Jan 2013; accepted 7 Jan 2013; published 8 Jan 2013